Electric Vehicle Charging Scheme for a Park-and-Charge System Considering Battery Degradation Costs

Zhe Wei, *Student Member, IEEE*, Yue Li, and Lin Cai, *Senior Member, IEEE*

***Abstract*—This paper studies the electric vehicle (EV) charging scheduling problem of a park-and-charge system with the objective to minimize the EV battery charging degradation cost while satisfying the battery charging characteristic. First, we design the operating model of the system while taking the interests of both customers and parking garage into consideration. Subsequently, a battery degradation cost model is devised to capture the characteristic of battery performance degradation during the charging process. Taking into account the developed battery degradation cost model, EV charging scheduling problem is explored and a cost minimization problem is formulated. To make the problem tractable, we investigate the features of the problem and decompose the problem into two subproblems. A vacant charging resource allocation algorithm and a dynamic power adjustment algorithm are proposed to obtain the optimal solution of cost minimization. Several simulations based on realistic EV charging settings are conducted to evaluate the effectiveness and applicability of the proposed methods in discussed charging scenarios. Simulation results exhibit the superior performance of the proposed algorithms in achieving the most degradation cost reduction and the lowest peak power load compared with other benchmark solutions, which is beneficial for both customers and charging operators.**

***Index Terms*—Battery degradation, capacity fading, electric vehicle charging, scheduling.**

NOMENCLATURE

α	Capacity fading rate function coefficient.
$\Delta\mathcal{C}$	Battery degradation cost reduction gain.
Δt	Time slot duration.
ϵ	A very small nuber.
B	Battery rated capacity.
E_a	Battery activation energy.
i	Task index.
K	Total available time slot number for a task for charging.
k	Charging time slot index.
L	Necessary required charging slot number for a task to reach objective battery SOC.
M	Total charger number.
N_t	Current active task number.
$\mathbf{P}$	Task charging power sequence.
$\mathbf{P}'$	Expanded charging power sequence.
R	Universal gas constant.
R_{th}	Thermal resistance of battery pack.
S^{ini}	Task initial battery SOC.
S^{obj}	Task objective battery SOC.
S^{th}	CC-CV period transition SOC threshold.
T	Total time slot number.
$\mathcal{T}$	Current battery temperature.
t	Current time slot.
t^a	Task arrival time.
t^d	Task departure time.
T_{amb}	Ambient temperature.
v	Available vacant time slot number for a task which can be used for expanding the charging sequence.
V	Total available vacant time slot number.
$\mathcal{C}(\bullet)$	Battery degradation cost function.
$P(S)$	Charging power function.
$\mathcal{P}(t)$	Time varying charging power function.
$r(\bullet)$	Battery capacity rate fading function.
$\mathcal{S}(t)$	Time varying SOC function.

Manuscript received November 6, 2017; revised March 5, 2018; accepted April 20, 2018. Date of publication June 1, 2018; date of current version August 23, 2018. This work was supported in part by the Natural Sciences and Engineering Research Council of Canada and in part by the China Scholarship Council. *(Corresponding author: Lin Cai.)*

The authors are with the Department of Electrical and Computer Engineering, University of Victoria, Victoria, BC V8W 3P6, Canada (e-mail: weizhe@uvic.ca; liyue331@uvic.ca; cai@ece.uvic.ca).

Source codes of this work are available at https://www.researchgate.net/publication/322962721.

Color versions of one or more of the figures in this paper are available online at http://ieeexplore.ieee.org.

Digital Object Identifier 10.1109/TIV.2018.2843126

I. INTRODUCTION

TRANSPORTATION system electrification could effectively relieve the energy dependence on fossil fuels and gradually reduce the greenhouse gas emissions [1]. The growing popularity of electric vehicle facilitates the establishment of a green and sustainable society. As EV's market share is increasing, more and more public charging facilities are required to provide charging services for EV customers. Recently, one promising operation mode, named park-and-charge system [2], [3], has been proposed for electric vehicle charging. The parking garage equips several charging points and provides both the parking and charging services. EVs can be charged during the parking period. Some projects have been carried out to explore the feasibility of this mode [4], [5]. Several European universities led by ETH have conducted the V-charge project to design automated valet parking and charging system to implement this operation mode [5]. It is anticipated that the future parking garages at office buildings, business districts and

airports can be operated in this mode. An important step to promote this charging mode to large scale is to develop effective and efficient charging load scheduling scheme.

Many research works have been conducted on designing effective charging scheduling algorithms for EV charging operation. Some efforts have been put on the power grid oriented issues, i.e., how to mitigate the potential impact on the power grid associated with large scale EV charging [6]–[9]. In [7], a decentralized algorithm is proposed to schedule the electric vehicle charging with the objective of flattening the grid load. A two-stage optimization method is proposed in [8] to minimize the network energy loss using smart charging and discharging of PHEVs. Other group of works utilized the control, scheduling, and optimization methods to focus on the EV user oriented issues, i.e., improve the EV user quality of service during the charging process. Optimal power allocation and EV arrival rate adjustment strategies are investigated in [10] to reduce the EV charging requirement blocking probability. In [11], the minimization of EV charging waiting time via scheduling charging activities spatially and temporally in a large-scale road network was investigated.

Although the EV charging scheduling problems have been discussed from different aspects in these works, one of the core problems for electric vehicle has not been fully addressed yet. A major factor preventing the proliferation of electric vehicle in current auto market is the high cost of EV batteries [12]. Ensuring the healthy and efficient operation of the battery and extending the battery lifetime is one of the most concerned points for each EV owner, also a very important issue valued greatly from the charging operating business's perspective. Many internal and external factors affect the battery performance [13]–[20]. One important factor is the battery capacity fading, which has significant effects on the battery lifetime[18]. Several research works have investigated the factors affecting the battery capacity fading. One important contributing factor is temperature. A genetic algorithm based PHEV charging profile optimization has been addressed in [19] to find the optimal energy cost and battery resistance growth. A capacity fading model for $LiFePO_4$ based on real operating conditions in electric vehicles was proposed in [14] and concluded that preventing the high temperature of the battery was important to optimize the battery lifetime. The cost of EV battery wear due to V2G application in power system was analyzed in [20]. The effect of ambient temperature on the battery degradation was considered in this work. Without a good control of the battery charging process, a larger charging power will generate more heat and thus increase the battery temperature, which deteriorates the EV battery capacity and lifetime. An intelligent charging system capable of estimating and minimizing these effects can potentially extend the battery lifetime and reduce the battery degradation. Therefore, to achieve the best operating mode, it is crucial for the system to develop effective charging scheduling scheme to minimize the battery degradation cost and reduce the system peak power load, which is the primary motivation of this work.

The main contributions of this work are fourfold. First, we design a feasible operating framework for the park-and-charge system charging operator to provide charging service and manage the charging process taking into account the interests of both business and charging customers, which makes our designed three layer operating structure distinctive and comprehensive. Second, We model the battery charging characteristic during the actual charging process and applied it into the charging scheduling design, which makes the scheduling decision more practical and feasible. Third, we build a battery degradation cost model to capture the characteristic of battery performance degradation during the charging process and propose a feasible charging scheme to adjust charging power so as to minimize the battery degradation cost. Meanwhile, it also effectively alleviates the system peak power load, which is desirable for the charging system operation. Last but not least, we employ the practical charging settings in the current EV charging market and evaluate the performance of the proposed scheduling scheme in comparison with other currently widely utilized benchmark scheduling algorithms. The simulation results verify the correctness and effectiveness of the proposed charging scheduling scheme. It also provides a good guideline to implement the proposed protocol.

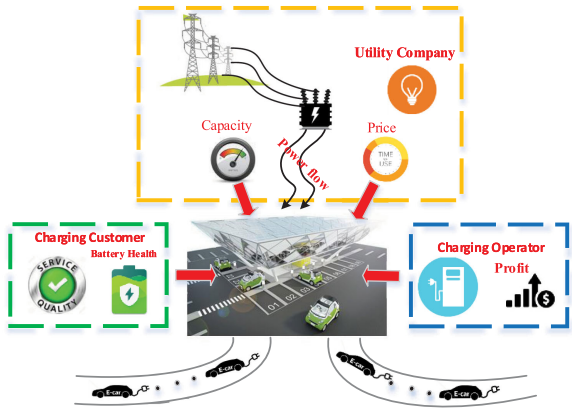

Fig. 1. Illustration of the park-and-charge system.

The remainder of this paper is organized as follows. The park-and-charge system and system models are introduced in Section II and III, respectively. In Section IV a battery degradation cost minimization problem is formulated and an optimal solution for the problem is proposed and analyzed in Section V. Simulation results are presented in Section VI, followed by the concluding remarks in Section VII.

II. Park-and-Charge System

In this section, we first propose a framework for the park-and-charge system and then further introduce the operating model of the designed system. The detailed implementation of the control strategy is introduced afterwards.

A. System Design

As illustrated in Fig. 1, in a large parking garage, every parking spot is equipped with a charging outlet and connected to the charging network. People drive to the parking garage, park their EVs, connect the vehicles to the charging outlets, and leave for

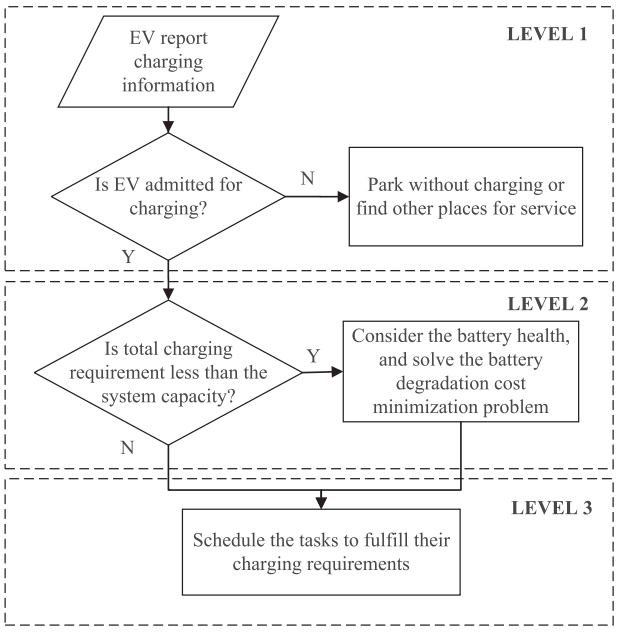

Fig. 2. Operation flow graph of the park-and-charge system.

their personal affairs, such as working, shopping and etc. During the parking period, the charging system can charge electricity to the connected EVs according to customer specified charging requirements. The park-and-charge system includes three participants: the utility company, the charging operator and the charging customers. The charging operator purchases electricity from the utility company and provide charging services to the customers. When an EV arrives at the parking garage, the driver reports the charging information, i.e., the arrival time, estimated departure time, current battery SOC and objective battery SOC, to the parking garage's charging management system (CMS). The CMS then makes a decision on whether to admit the customer's charging requirement based on its admission control mechanism. Each admitted vehicle's charging requirement must be satisfied before its departure time. All admitted vehicles are connected to the charging network to receive charging services. Those EVs with charging requirement rejected can park in the non-charging area or travel to other charging places for service. With the collected charging information of all admitted EVs, the CMS then distributes the optimal control strategy to schedule the charging activities of all admitted EVs to achieve the EV battery degradation cost minimization while ensuring all the admitted service requirements.

B. System Implementation

The designed park-and-charge system is operated in a top-down three-level structure as shown in Fig. 2. The top level implements the charging tasks admission control. It has the highest priority to guarantee the quality of service (QoS) for the arrived charging customers, i.e. the service opportunity and charging requirement fulfillment. Based on the customer reported charging information, the CMS can obtain the necessary required charging slot number and the corresponding charging sequence for each requested customer subject to the battery charging characteristics. Then, the CMS makes a decision on admitting or rejecting the charging requirement based on its admission control mechanism. After collecting the charging information of all admitted customers, the charging operator compares current total number of charging slots required with that are available. If they are equal, the charging operator determines the charging scheduling strategy directly based on the obtained charging sequences. Otherwise, the charging operator may use the vacant charging resources and adjust the charging power sequence for each customer to minimize the total battery degradation cost of all the charging customers and alleviate the system's peak power load at the same time. Then, the charging operator schedules the charging activities of all the active tasks based on their determined charging sequences.

III. System Models

In this section, we present the detailed system model applied to the designed park-and-charge system.

A. EV Mobility Model

Workplace parking garage is a typical implementation for a park-and-charge system. The employees can park their cars for charging during their normal working hours. After work they pick up their cars and drive back home. The charging service is usually provided during the working hours. The total charging service time per day is equally divided into T time slots with each slot duration as Δt. EVs dynamically arrive at the parking garage and are sequentially indexed according to their arrival time. Denote the ith EV's arrival time as t_i^a. The arrivals of EVs follow a Poisson process [11], [21], [22]. Considering the feature of a workplace parking garage, the EV departure time t_i^d can be assumed following a truncated Gaussian distribution [23] with the mean value as the peak leaving time. The dynamic departure case can be treated as a deadline restricted problem. Detailed discussion for the dynamic departure case can refer to our previous work [24]. To make the problem simpler, all vehicles are assumed to arrive at the beginning of each time slot, and depart at the end of the business day, i.e., time slot T.

B. Charging Requirement Model

When each EV arrives at the parking garage and requests charging service, the driver reports the EV's initial battery SOC S_i^{ini} and the objective battery SOC S_i^{obj} expected at the departure time to the CMS. Most users typically charge their EVs at the levels that were associated with the battery warnings [25]. The objective SOC of each EV depends on many factors such as the customer's expected staying time, charging rate and electricity price, etc. Accordingly, each EV's charging requirement can be regarded as a quadruple task, which is defined as follows

Definition 1: Assuming the ith EV arrives at the charging station at time t_i^a, and departs at time t_i^d, with its initial battery SOC as S_i^{ini} and objective battery SOC as S_i^{obj}. Each EV's charging requirement is parameterized by a quadruple vector $\mathbb{T}_i = (t_i^a, t_i^d, S_i^{ini}, S_i^{obj})$, which is defined as **Task** i**.**

C. Battery Charging Model

In current EV market, the major type of battery employed by the car manufacturers is Li-ion battery, which has better performances on capacity, safety, cost, etc., compared with the traditional lead acid battery and nickel metal hydride battery. For the Li-ion battery charging, constant-current constant-voltage (CC-CV) charging is the most widely utilized charging method [15], [26]. The charger varies the voltage applied to the battery to maintain a constant current flow at the CC period. When the voltage reaches the cell upper limit, it switches to the CV period where the charging voltage is maintained at that level. During the CV period due to the battery intrinsic electrochemical characteristic, the charging current decreases dramatically along with the increase of the battery SOC. The charging cut off occurs when a predetermined minimum current point, which indicates a full charge, has been reached.

To describe the relationship between the maximum allowable battery charging power and the battery SOC, we analyzed the Citroen C-Zero EV charging experimental measurements in [27] and obtained an approximate charging power function expressed as follows. EVs equipped with the same kind of batteries are considered subject to the same SOC function.

$$\mathscr{P}(S)=\begin{cases} P_0, & 0\le S\le S^{th},\\ \dfrac{1-S}{1-S^{th}}P_0, & S^{th}<S\le 1, \end{cases} \tag{1}$$

where S is the current battery SOC, S^{th} is the CC-CV period transition threshold. Since the voltage applied to the battery during the CC period changes not conspicuously, the charging power is approximated as a constant P_0 within this period. For the CV period, the charging power is approximated linearly decreasing with the growth of battery SOC.

Depending on each task's initial and objective battery SOCs, the battery charging process can be divided into the following three cases. The functions of battery SOC and charging power at any cumulative charging time t are expressed as follows, detailed derivation process can refer to [24].

Case 1: $S_i^{ini}\le S_i^{obj}\le S^{th}$.

The task's initial battery SOC is very low and only requires very few charging amount. In this case, the charging process only goes through the CC period. The battery charging power is maintained at the maximum level P_0. The task's battery SOC at any cumulative charging time t is expressed as

$$\mathcal{S}_i(t)=S_i^{ini}+\frac{P_0 t}{B}, \tag{2}$$

where B is the rated battery capacity of the electric vehicle.

Case 2: $0\le S_i^{ini}\le S^{th}\le S_i^{obj}$.

The charging process goes through both the CC and CV periods. The task's battery SOC at any cumulative charging time t is expressed as

$$\mathcal{S}_i(t)=\begin{cases} S_i^{ini}+\dfrac{P_0 t}{B}, & t\le t_i^{cc},\\ (S^{th}-1)e^{-\frac{P_0}{(1-S^{th})B}(t-t_i^{cc})}+1, & t>t_i^{cc}, \end{cases} \tag{3}$$

where $t_i^{cc}=\frac{(S^{th}-S_i^{ini})B}{P_0}$ is the task's charging duration for the CC period.

Substituting (3) into the function $\mathscr{P}(S)$ expressed in (1), the battery charging power function at any cumulative charging time thus can be obtained as

$$\mathcal{P}_i(t)=\begin{cases} P_0, & t\le t_i^{cc},\\ P_0 e^{-\frac{P_0}{(1-S^{th})B}(t-t_i^{cc})}, & t>t_i^{cc}. \end{cases} \tag{4}$$

Case 3: $S^{th}<S_i^{ini}\le S^{obj}\le 1$.

The charging process is deemed as only taking the CV period. The task's battery SOC at any cumulative charging time t is expressed as

$$\mathcal{S}_i(t)=(S^{th}-1)e^{-\frac{P_0}{(1-S^{th})B}(t+t_i^{cv})}+1, \tag{5}$$

where $t_i^{cv}=\frac{(1-S^{th})B}{P_0}\ln(\frac{1-S^{th}}{1-S_i^{ini}})$ is the duration when SOC changes from S^{th} to S_i^{ini} according to the SOC function.

Substituting (5) into the function $\mathscr{P}(S)$ expressed in (1), the battery charging power function at any cumulative charging time can be obtained as

$$\mathcal{P}_i(t)=P_0 e^{-\frac{P_0}{(1-S^{th})B}(t+t_i^{cv})}. \tag{6}$$

Given the equally divided time slot duration Δt, with each individual charging task's initial and objective battery SOCs S_i^{ini} and S_i^{obj}, its necessary required charging slot number L_i and the corresponding charging energy sequence $\mathbf{E}_i=\Big(E_i(1),E_i(2),\ldots,E_i(L_i)\Big)$ can be obtained by the SOC difference at each corresponding charging time slot, where L_i is the length of the energy sequence $\mathbf{E}_i$ and

$$\begin{aligned} E_i(k)&=\Big(\mathcal{S}_i(k\Delta t)-\mathcal{S}_i\big((k-1)\Delta t\big)\Big)\cdot B_i\\ &=\int_{(k-1)\Delta t}^{k\Delta t}\mathcal{P}_i(t)dt,\quad k=1,\ldots,L_i, \end{aligned} \tag{7}$$

Although the charging power varies continuously over time, while Δt is relatively small, the energy charging amount can be approximated as

$$E_i(k)\approx\mathcal{P}_i\Big((k-1)\Delta t\Big)\cdot\Delta t. \tag{8}$$

Then, to better describe a task's charging behavior we define the charging power sequence as follows

Definition 2: Given each task's initial and objective battery SOCs, according to the battery charging characteristic its charging power sequence $\mathbf{P}_i=\Big(P_i(1),\ldots,P_i(L_i)\Big)$ can be obtained, where $P_i(k)=\mathcal{P}_i\Big((k-1)\Delta t\Big)$ is the charging power at the beginning of the kth time slot, $k=1,\ldots,L_i$.

D. Battery Degradation Model

Capacity fading is an important manifestation of battery degradation. Experimental results [28] have shown that high temperature is a stress factor to accelerate the battery capacity fading. The temperature dependence of capacity fading rate can

be analyzed based on the Arrhenius relationship [29]:

$$r = Ae^{-E_a/(R\mathcal{T})}, \tag{9}$$

where r is the battery capacity fading rate under the absolute temperature $\mathcal{T}$ (in Kelvin), A is the proportionality constant, E_a is the activation energy, and R is the universal gas constant.

According to the Arrhenius relationship, it is noticeable that battery capacity fading rate increases exponentially as the temperature rises. During the EV charging process, with larger charging power, more heat is generated at the battery side. These generated heat will cause the battery temperature to rise, and then increase the battery capacity fading rate, which is unfavorable for the battery lifetime. According to the model proposed in [30], the temperature change produced by a given charging profile is approximated as a linear function of charging power expressed as

$$\mathcal{T}(P) = T_{amb} + R_{th} \cdot P, \tag{10}$$

where R_{th} is the thermal resistance of the battery pack and T_{amb} is the ambient temperature. Therefore, the relationship between the capacity fading rate and the charging power can be expressed as

$$r(P) = Ae^{-\frac{E_a}{R}\cdot\frac{1}{T_{amb}+R_{th}\cdot P}}. \tag{11}$$

It can be noticed that the larger the charging power the higher the battery temperature will be, which has more negative impact on the battery health and lifetime.

Given each task's charging power sequence $\mathbf{P}_i$, during the whole charging process the total generated battery capacity fading can be expressed as

$$Q_i = \sum_{k=1}^{L_i} r\Big(P_i\left(k\right)\Big)\Delta t. \tag{12}$$

Consequently, in order to optimize the charging profile and prolong the battery lifetime, estimated equivalent cost of battery degradation is defined here in terms of battery capacity fading, which is expressed as follows

$$\mathcal{C}(\mathbf{P}_i) = \frac{Q_i}{B_i}C_{bat} = \beta\sum_{k=1}^{L_i} r\Big(P_i\left(k\right)\Big), \tag{13}$$

where B_i is the rated battery capacity of task i, C_{bat} is the battery replacement cost, $\beta = \frac{\Delta t\cdot C_{bat}}{B_i}$ is a positive coefficient.

IV. Problem Formulation

As previously introduced in the system implementation part, the park-and-charge system is operated in an event-driven manner. The system schedules the electric vehicle charging activities in real-time. Detailed operation of the system is formulated as follows.

A. Task Admission Control

Whenever a new EV arrives at the parking garage and requests for charging, the CMS of the parking garage triggers the task admission control mechanism to determine if the charging requirement can be admitted for service. Considering current EV penetration rate and the service capability of the charging network, it is assumed that at most M EVs can be charged concurrently in the parking garage. For the newly arrived task $\mathbb{T}_j = (t_j^a, T, S_j^{ini}, S_j^{obj})$, given its charging information its necessary required charging slot number L_j and the corresponding charging power sequence $\mathbf{P}_j$ can be obtained accordingly. Then, the admission control mechanism makes the decision accordingly. A new task is accepted for charging if the following constraint is satisfied,

$$\sum_{i\in\mathbf{I}\left(t_j^a\right)} L_i^{t_j^a} + L_j^{t_j^a} \le M\left(T - t_j^a + 1\right), \tag{14}$$

where $\mathbf{I}\left(t_j^a\right)$ is the existing admitted active task set at time slot t_j^a, and $L_i^{t_j^a}$ is the necessary required charging slot number for each task in $\mathbf{I}$ at time slot t_j^a.

B. Battery Degradation Cost Minimization Problem

The admission control mechanism guarantees as many tasks as possible to get the charging opportunity under their acceptable maximum charging power conditions. While in most cases, especially under the low traffic scenarios, there are some vacant charging resources not being fully utilized if the vehicles are charged under their maximum acceptable charging power. Under these circumstances the charging operator can adjust the tasks' charging power and fully utilize all the vacant resources to minimize the battery degradation cost. Meanwhile, the system's peak power load is effectively relieved. Thus, a battery degradation cost minimization problem can be formulated as follows

$$\begin{aligned}
\mathbf{P_0}: \quad \min_{\mathbf{P}_i^t} \quad & \sum_{i=1}^{N_t}\mathcal{C}\left(\mathbf{P}_i^t\right) \\
\text{s.t.} \quad & P_i(1) \le \mathscr{P}\left(\mathcal{S}_i(t)\right), \\
& P_i(k) \le \mathscr{P}\left(\mathcal{S}_i(t) + \frac{1}{B_i}\sum_{j=1}^{k-1} P_i(j)\cdot\Delta t\right), k > 1 \\
& \sum_{k=1}^{L_i} P_i(k)\cdot\Delta t = \left(S_i^{obj} - \mathcal{S}_i(t)\right)\cdot B_i, \\
& \sum_i \mathbf{1}_{P_i(k)>0} \le M, \forall k.
\end{aligned} \tag{15}$$

The optimization problem is implemented in an event-driven manner, it is executed whenever a new task is admitted for charging. The charging operator adjusts the charging power sequence to minimize the total battery degradation cost of all the active tasks, where N_t in the objective function is the number of currently active tasks, $\mathbf{P}_i^t$ is the charging power sequence of task i at current time slot t. The first two constraints ensure that the active tasks' charging power at each charging time slot is smaller than their maximum allowable charging power following the battery charging characteristic, where $\mathcal{S}_i(t)$ is the battery SOC at the beginning of current time slot t. The third constraint guarantees the charging requirement fulfillment of each

admitted task after its whole charging process. The fourth constraint ensures that the number of EVs charged simultaneously cannot exceed the system maximum service capability, where $\mathbf{1}_{P_i(k)>0}$ is an indicator function.

V. Battery Degradation Cost Minimized EV Charging Scheme

By analyzing the feature of the above battery degradation cost minimization problem, it can be observed that we only need to adjust the task's charging power sequence under the situation that the total necessary required charging slot number is smaller than the available system service capacity.

According to the capacity fading rate function $r(\bullet)$, we can obtain the following Lemma.

Lemma 1: Within the feasible charging power range, the capacity fading rate function $r(\bullet)$ is convex.

Proof: See Appendix A. ■

As reducing the charging power is effective to slow down the battery capacity fading, a concept of expanding charging power sequence is defined as follows

Definition 3: Given the initial charging power sequence of task $\mathbb{T}_i$ as $\mathbf{P}_i = \Big(P_i(1), \ldots, P_i(L_i)\Big)$, by expanding the charging power sequence for v time slots, the updated charging power sequence is denoted as $\mathbf{P'}_i = \Big(P'_i(1), \ldots, P'_i(L_i), P'_i(L_i+1), \ldots, P'_i(L_i+v)\Big)$. The expanding procedure meets the following constraints

$$\sum_{k=1}^{L_i} P_i\left(k\right) = \sum_{k=1}^{L_i+v} P'_i\left(k\right), \tag{16}$$

and

$$P_i(k) \geq P'_i(k), \forall k \in [1, L_i]. \tag{17}$$

The first constraint guarantees the total charging requirement to remain unchanged after the expanding procedure. Under this premise, according to the battery charging characteristic the updated charging power is no larger than the original charging power at each specific charging time slot, which is indicated in the second constraint.

According to the convexity of the capacity fading rate function $r(\bullet)$ introduced by Lemma 1, we can further obtain the following properties.

Property 1: For any charging power P, it has the following relationship

$$r(P) \leq r'(P) \cdot P. \tag{18}$$

Proof: See Appendix B. ■

Property 2: For any charging power sequence $\mathbf{P}_i = \Big(P_i(1), \ldots, P_i(L_i)\Big)$, it has the following relationship

$$r'\Big(P_i(1)\Big) \geq r'\Big(P_i(2)\Big) \geq \cdots > r'\Big(P_i(L_i)\Big). \tag{19}$$

Proof: See Appendix C. ■

Property 3: For any charging power sequence element $P_i(k)$ and its counterpart $P'_i(k)$ in the expanded charging power sequence $\forall k \in [1, L_i]$, it has the following relationship

$$r\Big(P_i(k)\Big) \geq r\Big(P'_i(k)\Big) + r'\Big(P'_i(k)\Big)\Big(P_i(k) - P'_i(k)\Big). \tag{20}$$

Proof: See Appendix D. ■

Based on the above introduced properties, we can further obtain the following theorem,

Theorem 1: For any active task, expanding the charging power sequence is beneficial to decrease the battery degradation cost.

Proof: See Appendix E. ■

According to Theorem 1, it is beneficial to make full use of all the available charging resources to reduce the total battery degradation cost. Given the updated total charging slot number K for each specific task, we need to determine its charging power sequence accordingly to minimize the cost while satisfying all charging constraints. Thus, the problem can be expressed as

$$\begin{aligned}
\mathbf{P_1}: \quad & \min_{P(k)} \quad \sum_{k=1}^{K} r\Big(P(k)\Big) \\
& \text{s.t.} \quad P(1) \leq \mathscr{P}\Big(\mathcal{S}\left(t\right)\Big) \\
& P(k) \leq \mathscr{P}\left(\mathcal{S}\left(t\right) + \frac{1}{B}\sum_{j=1}^{k-1} P(j)\cdot\Delta t\right), k > 1 \\
& \sum_{k=1}^{K} P(k)\cdot\Delta t = \Big(S^{obj} - \mathcal{S}\left(t\right)\Big)\cdot B
\end{aligned} \tag{21}$$

where $K = \min(L+v, T)$, L is the task's necessary required charging slot number at current time slot t, and v is the extra available vacant charging slot number which can be allocated to the task for charging. The first two constraints in the optimization problem restricts the charging power at each time slot not exceeding the maximum allowable charging power as per the battery charging characteristic. The third constraint restricts the task's charging requirement being satisfied after the whole charging duration.

Given the extra available vacant charging slot number v, we propose a dynamic power adjustment algorithm (DPA) to solve the above problem $\mathbf{P_1}$. Detailed description of the DPA algorithm is depicted in Algorithm 1. For the task whose S^{obj} is smaller than S^{th}, by expanding the charging sequence, the power is evenly distributed throughout the whole charging process. For other tasks, there is an iterated process to obtain the feasible charging power sequence. We first set a base charging power P_1 evenly distributed among all available charging slots as step 8 shows. Since the battery maximum allowable charging power gradually decreases with the increase of battery SOC, if the EV is always charged in accordance with the base charging power P_1, it will break the maximum allowable charging power constraint in the later charging phase as illustrated in Fig. 3. In other words, in real charging process the charging activity still follows the physical maximum charging power constraint. However, due to the small charging power allocated at the beginning of the charging process, the customer specified charging

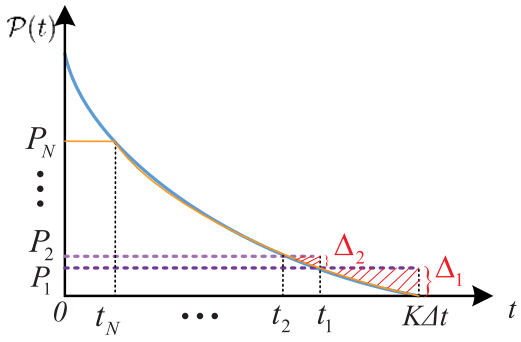

Fig. 3. Illustration of Algorithm 1.

Algorithm 1: Dynamic Power Adjustment Algorithm.

Input: S^{ini}, S^{obj}, L, v, ϵ

1: $K = \min(L+v, T)$
2: **if** $S^{obj} \le S^{th}$ **then**
3: $P'(k) = \frac{(S^{obj}-S^{ini})B}{K\Delta t}, k = 1, \ldots, K$
4: **else**
5: $P_0 = \mathscr{P}(S^{ini})$
6: Get the task's charging power curve $\mathcal{P}(t)$ by P_0, S^{ini}
7: Set $i = 1$
8: Obtain the initial charging power $P_i = \frac{(S^{obj}-S^{\text{int}})B}{K\Delta t}$
9: Get $t_i = \mathcal{P}^{-1}(P_i)$
10: Get $\Delta_i = P_i \cdot (K\Delta t - t_i) - \int_{t_i}^{K\Delta t} \mathcal{P}(t)dt$
11: **while** $\Delta_i > \epsilon$ **do**
12: $i = i + 1$
13: $P_i = P_{i-1} + \frac{\Delta_{i-1}}{t_{i-1}}$
14: $t_i = \mathcal{P}^{-1}(P_i)$
15: $\Delta_i = P_i \cdot (t_{i-1} - t_i) - \int_{t_i}^{t_{i-1}} \mathcal{P}(t)dt$
16: **end while**
17: Get $t' = \mathcal{P}^{-1}(P_i)$
18: $P(t) = P_i$, for $t \in [0, t']$
19: $P(t) = \mathcal{P}(t)$, for $t \in [t', K\Delta t]$
20: $P'(k) = P\big((k-1)\Delta t\big), k = 1, \ldots, K$
21: **end if**

Output: Updated charging power sequence $\mathbf{P}'$

requirement cannot be fully satisfied at the end of the charging process. There will be a charging amount shortage Δ as the red shaded area shows in Fig. 3. Thus, the charging power needs to be adjusted iteratively until the feasible charging power sequence is obtained. The detailed power adjustment procedure is shown in steps 11 to 16. At last, we can obtain the updated charging power sequence $\mathbf{P}'$, which guarantees to minimize the battery degradation cost for the given task while satisfying all the charging constraints.

Problem $\mathbf{P_1}$ achieves the cost minimization for each individual task given its total available charging slot number K. However, for the whole charging system we need to determine how to allocate all the vacant resources to the corresponding tasks so as to minimize the total battery degradation cost of the system as the original problem $\mathbf{P_0}$ indicates. According to Theorem 1, it can be noted that expanding the charging sequence

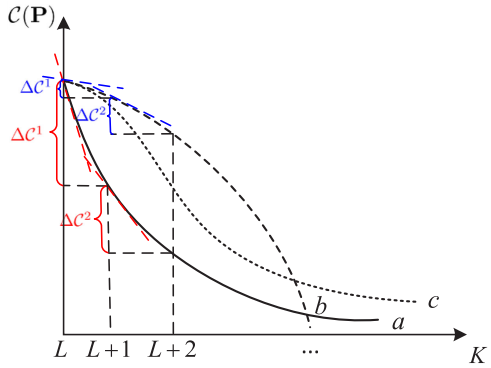

Fig. 4. Illustration of the cost function by expanding charging sequence.

can effectively reduce the battery degradation cost $\mathcal{C}$. We focus on how the cost reduction amount changes by successively expanding the charging sequence over one more vacant charging resource of each individual task. The cost reduction gain is expressed as follows

$$\Delta\mathcal{C}^v = \mathcal{C}(\mathbf{P}^{v+1}) - \mathcal{C}(\mathbf{P}^v), v = 0, 1, \ldots \tag{22}$$

where $\mathbf{P}^v$ is updated charging power sequence after expanding the original charging power sequence over v time slots.

As illustrated in Fig. 4, there are three possibilities for the cost reduction trend by expanding the charging sequence. For case a, the cost reduction gain $\Delta\mathcal{C}^v$ by successively expanding the charging sequence over one more time slot is gradually decreasing. Thus, the vacant charging resources can be allocated individually to the task which produces the most cost reduction to achieve the maximum cost saving for the system. While for case b, the cost reduction gain $\Delta\mathcal{C}^v$ by successively expanding the charging sequence over one more time slot is gradually increasing. Therefore, the vacant charging resources can be preferentially allocated to the task which makes the most cost reduction to its maximum extent, so on so forth until all vacant charging resources have been allocated. For case c, since how the cost reduction gain $\Delta\mathcal{C}^v$ exactly changes is uncertain, it is difficult to obtain the optimal allocation solution directly.

To determine how to allocate the resources, we need to investigate the probability of $Pr\{\Delta\mathcal{C}^{v+1} < \Delta\mathcal{C}^v\}$. Owing to the unavailability of the explicit expression of the charging power sequence, it's hard to obtain the probability from mathematical derivations. Consequently, we conduct 5000 Monte-Carlo simulations to evaluate $Pr\{\Delta\mathcal{C}^{v+1} < \Delta\mathcal{C}^v\}$ with different values of the battery degradation cost parameter α. Simulation result is shown in Fig. 5. Under the feasible value of $\alpha = 5740$ °C (6013.6 K), we can see $Pr\{\Delta\mathcal{C}^{v+1} < \Delta\mathcal{C}^v\} = 1$, which means for any task by successively expanding the charging power sequence the cost reduction gain is decreasing like case a indicates in Fig. 4.

According to the above discussed feature, we propose an optimal vacant resource allocation algorithm (VRA), as described in Algorithm 2, to allocate all these vacant charging resources to the best candidates to minimize the total battery degradation cost of the system. Assuming there are V available vacant

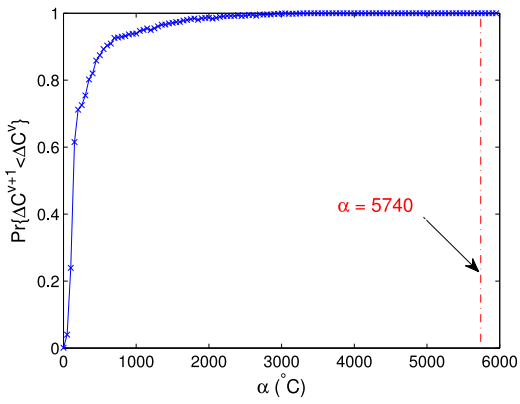

Fig. 5. $Pr\{\Delta\mathcal{C}^{v+1} < \Delta\mathcal{C}^{v}\}$ vs. α.

Algorithm 2: Vacant Resource Allocation Algorithm.

Input: t, $\mathbf{I}$, $\mathbf{S^t}$, $\mathbf{S^{obj}}$, ϵ, V

Obtain each task's current charging power sequence $\mathbf{P}_i$ and the sequence length $L_i^0 = \|\mathbf{P}_i\|_{\ell_0}, i \in \mathbf{I}$
while $V > 0$ **do**
  for $i = 1 : \|\mathbf{I}\|_{\ell_0}$ **do**
    $L_i = \|\mathbf{P}_i\|_{\ell_0}$
    if $0 < L_i < T - t + 1$ **then**
      $\mathbf{P'}_i = \mathrm{DPA}(S_i^t, S_i^{obj}, L_i^0, L_i + 1 - L_i^0, \epsilon)$
      $\Delta\mathcal{C}_i = \mathcal{C}(\mathbf{P}_i) - \mathcal{C}(\mathbf{P'}_i)$
    else $\Delta\mathcal{C}_i = 0$
    end if
  end for
  if $\max(\boldsymbol{\Delta\mathcal{C}}) = 0$ **then**
    break
  end if
  $[\Delta\mathcal{C}_k, k] = \arg\max \boldsymbol{\Delta\mathcal{C}}$
  $\mathbf{P}_k = \mathbf{P'}_k$
  $V = V - 1$
end while

Output: The updated charging power sequence $\mathbf{P}_i, i \in \mathbf{I}$

charging resources besides all tasks' necessary required charging requirements. The V resources are allocated individually. We hypothetically expand each task's charging sequence for one time slot and obtain its updated charging power sequence by solving problem $\mathbf{P}_1$. Then, the cost reduction gain $\Delta\mathcal{C}$ of each task after expanding the charging sequence can be obtained. By comparing the potential cost reduction gain of all the tasks, we can find the one which produces the maximum cost reduction. Then, this vacant charging resource is allocated to this task and its charging sequence is updated correspondingly. This procedure is iteratively executed until all V resources have been allocated. For each specific task its maximum charging sequence length cannot be larger than the total available slot number from current time to the end of the business day. If any task reaches this limit, it will not be engaged in the allocation anymore.

Based on the feature of cost reduction gain $\Delta\mathcal{C}^v$, for the proposed greedy based vacant resource allocation algorithm we can obtain the following theorem,

Theorem 2: The proposed vacant resource allocation algorithm is optimal to achieve the minimum battery degradation cost for the system.

Proof: See Appendix F. ■

Ultimately, according to the determined charging power sequence of each active task, the charging operator makes the scheduling decision for each time slot. As the system is operated in an event-driven manner, whenever a new task arrives, it needs to reallocate the charging resources and update each task's charging profile. Thus, it's better to schedule the larger charging power task first to save more charging resources and leave more flexibility to serve the future arrived charging requirements.

VI. Performance Evaluation

In this section, we conduct extensive simulations to evaluate the performance of the proposed battery degradation cost minimized charging scheme by comparing it with two widely applied benchmark strategies Round-Robin [31], [32] and Random [6], [33]. All results are carried out over 500 Monte Carlo simulations.

A. Simulation Setting

We take a regular workplace parking garage as the object. The whole working hours (9am–5pm) are equally divided into $T = 800$ time slots, with each slot duration as $\Delta t = 0.01$ hrs. Considering the current EV penetration rate and the grid configuration in a workplace parking garage, we assume at most $M = 8$ EVs can be charged simultaneously [34] in the garage. To demonstrate the wide range applicability and robust performance of the proposed charging scheme, three different charging scenarios are studied here: Case 1, all EVs are homogeneously equipped with the same type of battery, they arrive before work and depart after work. This case can be treated as an offline case, all tasks' charging information are known to the charging operator. Case 2, all settings are the same as Case 1 except that the arrived EVs are heterogeneously equipped with two different types of batteries. Case 3, the EVs dynamically arrive at the parking garage before the middle of the day following a Poisson process with an arrival rate λ and depart after work. This case can be treated as an online case, the task's charging information reveals to the charging operator only when it arrives at the parking garage. For Case 1 and 3, EVs are equipped with $B = 60$ kWh batteries. The battery CC-CV stage transition threshold is $S^{th} = 0.6$. For Case 2, half of the vehicles are equipped with $B = 60$ kWh batteries with the $S^{th} = 0.6$, the other half are equipped with $B = 80$ kWh batteries with the $S^{th} = 0.7$. For all cases, The maximum charging power during the CC stage is $P_0 = 40$ kW. The parameter $\epsilon = 10^{-4}$. Considering the charging behaviours of most customers, the initial EV battery SOCs S^{ini} are assumed following a uniform distribution from 0.1 to 0.5. The required battery SOCs S^{obj} are assumed following a uniform distribution from 0.8 to 0.9 as many electric

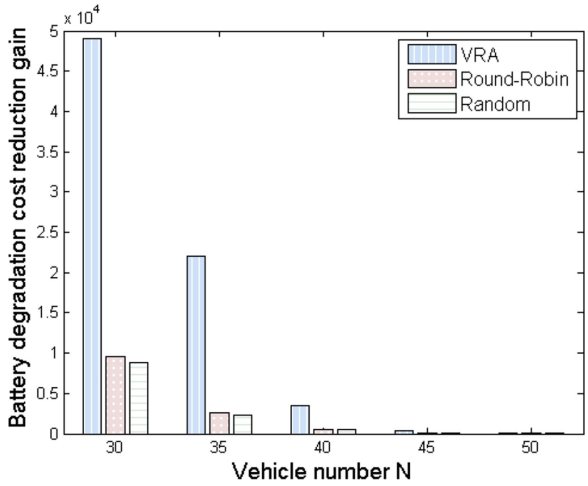

Fig. 6. Homo-battery case total battery degradation cost reduction gain.

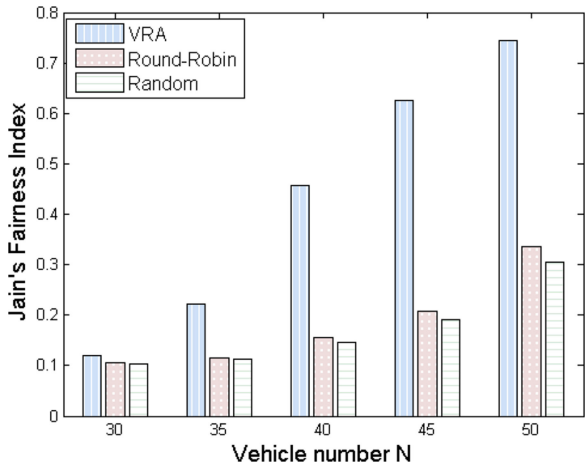

Fig. 7. Homo-battery case Jain's fairness index.

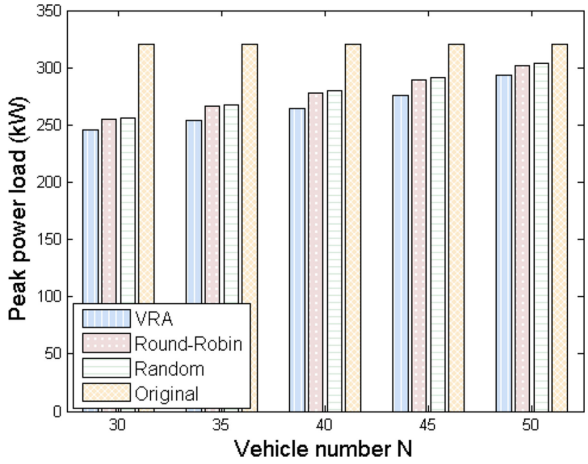

Fig. 8. Homo-battery case peak charging power load.

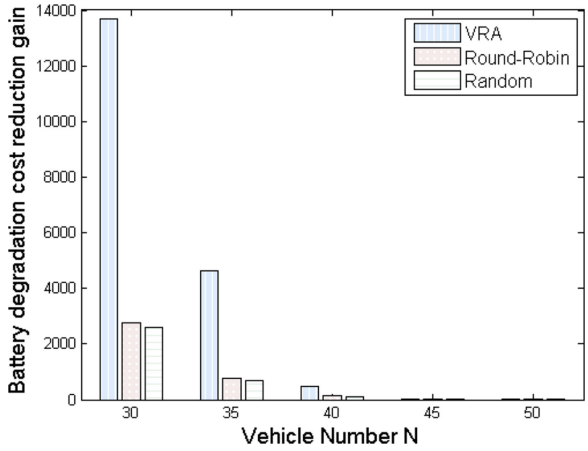

Fig. 9. Het-battery case total battery degradation cost reduction gain.

vehicle manufactures recommend the users note necessary to fully charge the battery to prolong the battery lifetime [35].

B. Simulation Results

For Case 1 the offline scenario, the performance of battery degradation cost reduction gain over the original unexpanded case under different arrived vehicle numbers is first demonstrated in Fig. 6. From the figure, we can see by utilizing the vacant charging resources the battery degradation cost are significantly reduced. With more vehicles arriving there are less vacant charging resources can be utilized, thus the cost reduction gain is correspondingly decreased. However, our proposed VRA algorithm can always achieve the best cost reduction gain compared with the other two strategies.

In order to evaluate the fairness issue among all the charging customers under different allocation strategies, we employ the Jain's fairness index [36], which is defined as follows

$$\mathcal{J}\left(C_1, C_2, \ldots, C_N\right) = \frac{\left(\sum_{i=1}^{N} C_i\right)^2}{N \cdot \sum_{i=1}^{N} C_i^2}, \tag{23}$$

where N is the total charging customer number, $C_i = \mathcal{C}(\mathbf{P}_i)$ is the battery degradation cost of the ith customer. The fairness comparison is shown in Fig. 7. It can be noticed that VRA algorithm achieves the best fairness for all customers to reduce their battery degradation cost.

As we discussed before, expanding the charging sequence can not only reduce the battery degradation cost, which is beneficial for the customers to prolong the battery lifetime, it is also effective to relieve the peak load for the charging system. The peak charging power load comparison under 40 arriving vehicles case is shown in Fig. 8. It can be noted that with using the VRA algorithm the system peak charging power load reduces the most 15% among all the algorithms under the discussed scenario, which is very promising for the charging system operation.

For Case 2, we would like to verify the proposed charging scheme can be applied to the heterogeneous battery case as well. The performance of battery degradation cost reduction gain, Jain's fairness index and peak power load under different arrived vehicle number cases are compared in Figs. 9–11, respectively. From the simulation results, it can be observed that the proposed VRA algorithm still achieves the most battery degradation cost reduction gain, the best fairness, and the most

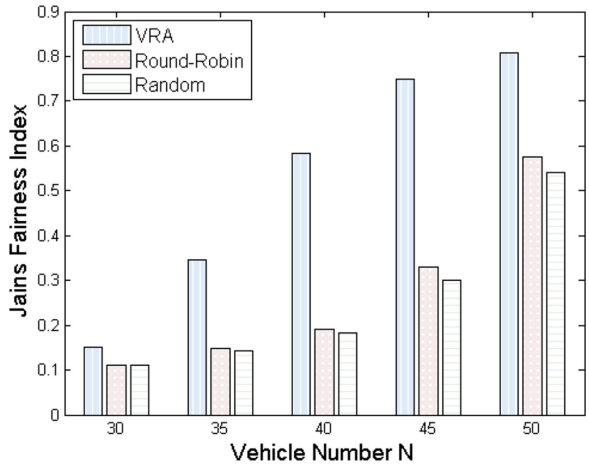

Fig. 10. Het-battery case Jain's fairness index.

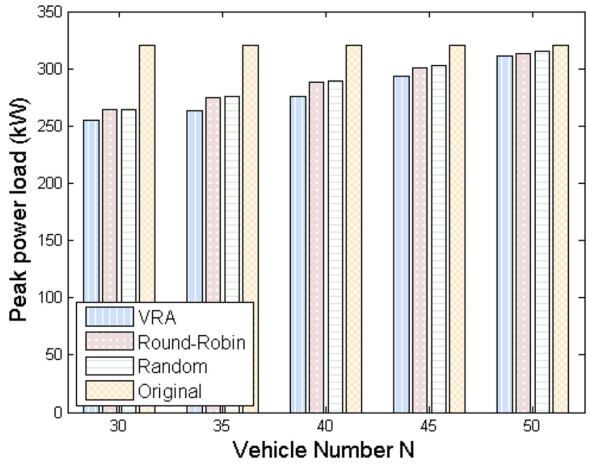

Fig. 11. Het-battery case peak charging power load.

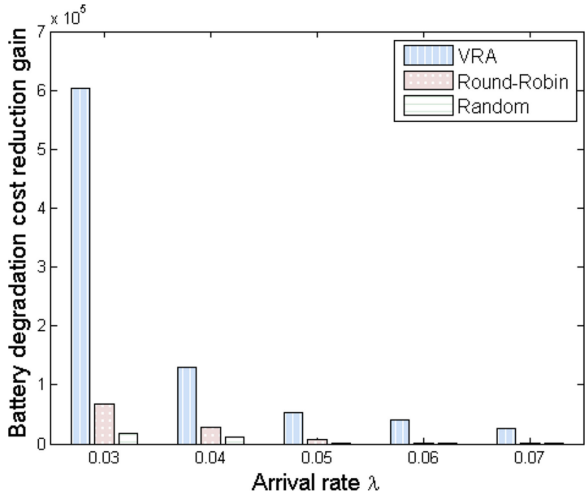

Fig. 12. Online case total battery degradation cost reduction gain.

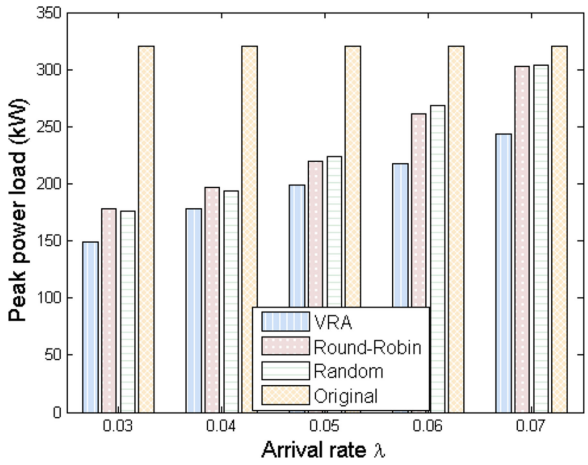

Fig. 13. Online case peak charging power load.

peak power load alleviation in comparison with the other two solutions. Therefore, the proposed charging scheme demonstrates wide range applicability and effectiveness, which benefits both the customers and charging operator.

For Case 3 the online scenario, all EVs dynamically arrive at the parking garage. To verify the effectiveness and robustness of the proposed charging scheme, we evaluate the performance under different arrival rate scenarios. The battery degradation cost reduction gain over the original unexpanded case is compared in Fig. 12. From the figure, we can see the proposed VRA algorithm can always achieve the most battery degradation cost reduction among all the strategies. Another important performance index, system peak power load, is demonstrated in Fig. 13. With increasing the arrival rate, there are higher probability more vehicles are charged simultaneously, which will make the system peak load rise. By utilizing our proposed VRA algorithm, it can be noted that the system power load can be always effectively decreased. Under some scenarios, the system peak power can be reduced over 50 $\%$ compared with the original unexpanded case, which is quite promising for the charging system operation.

VII. Conclusion

In this paper, we investigated the EV charging problem under a park-and-charge system. We designed the operating model for the system to provide charging service by jointly considering the interests of both customers and business. A practical charging scheme was proposed for integrating the effects of battery degradation into EV charging scheduling problem. We devised a battery degradation cost model to capture the characteristic of battery performance degradation during the charging process. The developed battery degradation cost model was incorporated into the optimal EV charging scheduling scheme design to minimize the system total battery degradation cost. By investigating the feature of the cost minimization problem, we decomposed the problem into two sub-problems and proposed vacant resource allocation algorithm and dynamic power adjusting algorithm to solve the associated optimization problem. The applicability and effectiveness of the proposed methods were demonstrated through several case studies. The obtained results exhibited the superior performance of the proposed method in achieving both battery degradation cost minimization and

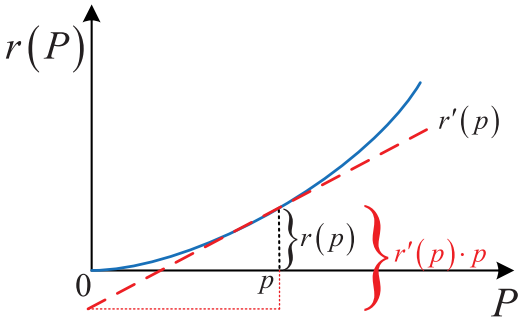

Fig. 14. Illustration for Property 1.

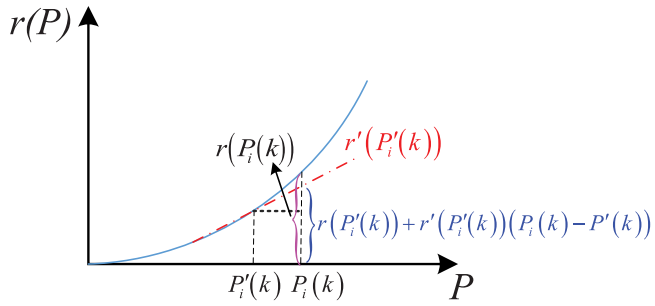

Fig. 15. Illustration for Property 3.

system peak power load reduction, which benefits both the customers and charging operator.

Appendix A
Proof of the Lemma 1

Proof: According to (11), the capacity fading rate function can be written as $r(P) = ae^{-\alpha \cdot \frac{1}{k_1 P + b}}$, where $a = A$, $\alpha = \frac{E_a}{R}$, $k_1 = R_{th}$, $b = T_{amb}$ are all positive coefficients.

Then, we can obtain

$$\frac{\partial r}{\partial P} = a\alpha k_1 \cdot \frac{1}{(k_1 P + b)^2} \cdot e^{-\frac{\alpha}{k_1 P + b}} > 0, \tag{24}$$

$$\frac{\partial^2 r}{\partial P^2} = a\alpha k_1^2 \cdot e^{-\frac{\alpha}{k_1 P + b}} \cdot \left[\frac{\alpha}{(k_1 P + b)^4} - \frac{2}{(k_1 P + b)^3} \right]. \tag{25}$$

It can be seen that the convexity of $r(P)$ depends on the relationship between P and $\frac{(\alpha/2 - b)}{k_1}$. When $P < \frac{(\alpha/2 - b)}{k_1}$, the capacity fading rate function is convex. According to the measurement data by Sandia National Laboratories, the Li-ion battery has an activation energy on the order of 50 kJ/mol [37]. The universal gas constant $R = 8.3144598$ J/mol/K. Thus, $\alpha = E_a/R = 6013.6$ K (5740 °C). The thermal resistant $R_{th} = 0.002$ °C/W, and the ambient temperature is 25 °C [30]. According to the current charging technology, the maximum charging power P is around 120 kW [34], which is far smaller than the value of $\frac{(\alpha/2 - b)}{k_1}$. Then, we can see $\frac{\partial^2 r}{\partial P^2} > 0$. Thus, within the feasible charging power range the capacity fading rate function $r(\bullet)$ is convex. ■

Appendix B
Proof of the Property 1

Proof: This property can be easily derived according to the feature of a convex function. An illustration of this property is shown in Fig. 14. ■

Appendix C
Proof of the Property 2

Proof: According to Lemma 1, we have known $\frac{\partial^2 r}{\partial P^2} > 0$. Thus, $r'(\bullet)$ is an increasing function. Since the charging power sequence has a decreasing trend in accordance with the battery charging characteristic, i.e. $P_i(1) \geq P_i(2) \geq \cdots \geq P_i(L_i)$, we can obtain the given relationship. ■

Appendix D
Proof of the Property 3

Proof: Based on Lemma 1, we have known that $r(\bullet)$ is a convex function. Given $P_i(k) \geq P'_i(k), \forall k \in [1, L_i]$, according to the property of convex function we have

$$\begin{aligned} r\Big(P_i(k)\Big) &= r\Big(P'_i(k) + P_i(k) - P'_i(k)\Big) \\ &\geq r\Big(P'_i(k)\Big) + r'\Big(P'_i(k)\Big)\Big(P_i(k) - P'_i(k)\Big). \end{aligned} \tag{26}$$

This relationship can also be observed from the illustration example shown in Fig. 15. ■

Appendix E
Proof of the Theorem 1

Proof: Denote the original charging power sequence as $\mathbf{P}_i = \Big(P_i(1), \ldots, P_i(L_i)\Big)$. By expanding the power sequence for one time slot, the updated charging power sequence is denoted as $\mathbf{P'}_i = \Big(P'_i(1), \ldots, P'_i(L_i + 1)\Big)$. According to the definition of battery degradation cost in (13) and Property 3, we have

$$\begin{aligned} \mathcal{C}(\mathbf{P}_i) &= \beta \sum_{k=1}^{L_i} r\Big(P_i(k)\Big) \\ &= \beta \sum_{k=1}^{L_i} r\Big(P'_i(k) + P_i(k) - P'_i(k)\Big) \\ &\geq \beta \left(\sum_{k=1}^{L_i} r\Big(P'_i(k)\Big) + r'\Big(P'_i(k)\Big)\Big(P_i(k) - P'_i(k)\Big) \right). \end{aligned} \tag{27}$$

Based on the definition of power sequence expanding, we have

$$\sum_{k=1}^{L_i} \Big(P_i(k) - P'_i(k)\Big) = P'_i(L_i + 1). \tag{28}$$

According to Properties 1 and 2, we have

$$r\Big(P'_i(L_i + 1)\Big) \leq r'\Big(P'_i(L_i + 1)\Big) \cdot P'_i(L_i + 1), \tag{29}$$

and

$$r'\Big(P_i'(1)\Big) \geq r'\Big(P_i'(2)\Big) \geq \cdots \geq r'\Big(P_i'(L_i+1)\Big). \quad (30)$$

Then, we have

$$\begin{aligned} r\Big(P'_i(L_i+1)\Big) &\leq r'\Big(P'_i(L_i+1)\Big)\cdot P'_i(L_i+1) \\ &= r'\Big(P'_i(L_i+1)\Big)\cdot \sum_{k=1}^{L_i}\Big(P_i(k)-P'_i(k)\Big) \\ &\leq \sum_{k=1}^{L_i} r'\Big(P'_i(k)\Big)\cdot\Big(P_i(k)-P'_i(k)\Big). \end{aligned} \quad (31)$$

Thus,

$$\begin{aligned} C(\mathbf{P}_i) &\geq \beta\left(\sum_{k=1}^{L_i} r\Big(P'_i(k)\Big) + r'\Big(P'_i(k)\Big)\Big(P_i(k)-P'_i(k)\Big)\right) \\ &\geq \beta\left(\sum_{k=1}^{L_i} r\Big(P'_i(k)\Big) + r\Big(P'_i(L_i+1)\Big)\right) \\ &= \beta\sum_{k=1}^{L_i+1} r\Big(P'_i(k)\Big) = C(\mathbf{P}'_i). \end{aligned} \quad (32)$$

Similar way works for expanding the power sequence for more time slots. Therefore, it can be seen expanding the power sequence can effectively decrease the battery degradation cost.

Appendix F: Proof of the Theorem 2

Proof: From the original charging power sequence, successively expanding the sequence over one more time slot, according to the definition of $\Delta\mathcal{C}$, denote the battery degradation cost reduction gain sequence of task i as $\boldsymbol{\Delta\mathcal{C}}_i = \big[\Delta\mathcal{C}_i^1, \Delta\mathcal{C}_i^2, \ldots, \Delta\mathcal{C}_i^v, \cdots\big]$, where $\Delta\mathcal{C}_i^{v+1} < \Delta\mathcal{C}_i^v, \forall v = 1, 2, \cdots$.

Assuming in current step, we need to allocate resources to the active candidate tasks $m, n, q, \cdots$ with their current corresponding battery degradation cost reduction sequences as $\boldsymbol{\Delta\mathcal{C}}_m = \big[\Delta\mathcal{C}_m^M, \Delta\mathcal{C}_m^{M+1}, \cdots\big]$, $\boldsymbol{\Delta\mathcal{C}}_n = \big[\Delta\mathcal{C}_n^N, \Delta\mathcal{C}_n^{N+1}, \cdots\big]$, $\boldsymbol{\Delta\mathcal{C}}_q = \big[\Delta\mathcal{C}_q^Q, \Delta\mathcal{C}_q^{Q+1}, \cdots\big], \cdots$.

Assuming in this step, we allocate the resource to task n, where $\Delta\mathcal{C}_n^N = \max\big\{\Delta\mathcal{C}_n^N, \Delta\mathcal{C}_m^M, \Delta\mathcal{C}_q^Q, \cdots\big\}$. Then, in the next step we will allocate the resource to task i^*, where $\Delta\mathcal{C}_{i^*}^{(\cdot)} = \max\big\{\Delta\mathcal{C}_n^{N+1}, \Delta\mathcal{C}_m^M, \Delta\mathcal{C}_q^Q, \cdots\big\}$.

Hypothetically, the greedy based vacant resource allocation algorithm is not optimal, there must exist an optimal solution satisfying $\Delta\mathcal{C}_m^{M+1} > \Delta\mathcal{C}_{i^*}^{(\cdot)}$ or $\Delta\mathcal{C}_q^{Q+1} > \Delta\mathcal{C}_{i^*}^{(\cdot)}$, or $\cdots$, which means $\Delta\mathcal{C}_m^{M+1} > \Delta\mathcal{C}_m^M$, or $\Delta\mathcal{C}_q^{Q+1} > \Delta\mathcal{C}_q^Q, \cdots$. Obviously, this is contradicted to the actual condition for any task i $\Delta\mathcal{C}_i^{v+1} < \Delta\mathcal{C}_i^v, \forall v = 1, 2, \cdots$.

Thus, we can see the hypothesis does not hold. The greedy solution is actually optimal. ■

References

[1] N. Chen, C. W. Tan, and T. Q. Quek, "Electric vehicle charging in smart grid: Optimality and valley-filling algorithms," *IEEE J. Sel. Topics Signal Process.*, vol. 8, no. 6, pp. 1073–1083, Dec. 2014.

[2] Q. Xiang, F. Kong, X. Liu, X. Chen, L. Kong, and L. Rao, "Auc2Charge: An online auction framework for electric vehicle park-and-charge," in *Proc. ACM 6th Int. Conf. Future Energy Syst.*, 2015, pp. 151–160.

[3] F. Kong, Q. Xiang, L. Kong, and X. Liu, "On-line event-driven scheduling for electric vehicle charging via park-and-charge," in *Proc. IEEE Real-Time Syst. Symp.*, 2016, pp. 69–78.

[4] 2014. [Online]. Available: http://timberrockes.com/docs/TRES-MEA.pdf

[5] U. Schwesinger *et al.*, "Automated valet parking and charging for e-mobility-results of the V-charge project," in *Proc. IEEE Intell. Veh. Symp.*, 2016, pp. 157–164.

[6] S. Deilami, A. S. Masoum, P. S. Moses, and M. A. Masoum, "Real-time coordination of plug-in electric vehicle charging in smart grids to minimize power losses and improve voltage profile," *IEEE Trans. Smart Grid*, vol. 2, no. 3, pp. 456–467, Sep. 2011.

[7] L. Gan, U. Topcu, and S. H. Low, "Optimal decentralized protocol for electric vehicle charging," *IEEE Trans. Power Syst.*, vol. 28, no. 2, pp. 940–951, May 2013.

[8] H. Nafisi, S. M. M. Agah, H. A. Abyaneh, and M. Abedi, "Two-stage optimization method for energy loss minimization in microgrid based on smart power management scheme of PHEVs," *IEEE Trans. Smart Grid*, vol. 7, no. 3, pp. 1268–1276, May 2016.

[9] A. Y. Lam, K.-C. Leung, and V. O. Li, "Capacity estimation for vehicle-to-grid frequency regulation services with smart charging mechanism," *IEEE Trans. Smart Grid*, vol. 7, no. 1, pp. 156–166, Jan. 2016.

[10] I. S. Bayram, G. Michailidis, M. Devetsikiotis, and F. Granelli, "Electric power allocation in a network of fast charging stations," *IEEE J. Sel. Areas Commun.*, vol. 31, no. 7, pp. 1235–1246, Jul. 2013.

[11] H. Qin and W. Zhang, "Charging scheduling with minimal waiting in a network of electric vehicles and charging stations," in *Proc. 8th ACM Int. Workshop Veh. Inter-Netw.*, 2011, pp. 51–60.

[12] A. Hoke, A. Brissette, D. Maksimović, A. Pratt, and K. Smith, "Electric vehicle charge optimization including effects of lithium-ion battery degradation," in *Proc. IEEE Veh. Power Propulsion Conf.*, 2011, pp. 1–8.

[13] H. Farzin, M. Fotuhi-Firuzabad, and M. Moeini-Aghtaie, "A practical scheme to involve degradation cost of lithium-ion batteries in vehicle-to-grid applications," *IEEE Trans. Sustain. Energy*, vol. 7, no. 4, pp. 1730–1738, Oct. 2016.

[14] L. Lam and P. Bauer, "Practical capacity fading model for Li-ion battery cells in electric vehicles," *IEEE Trans. Power Electron.*, vol. 28, no. 12, pp. 5910–5918, Dec. 2013.

[15] L. He, Y.-C. Tung, and K. G. Shin, "iCharge: User-interactive charging of mobile devices," in *Proc. 15th Annu. Int. Conf. Mobile Syst., Appl., Serv.*, 2017, pp. 413–426.

[16] K. Onda, T. Ohshima, M. Nakayama, K. Fukuda, and T. Araki, "Thermal behavior of small lithium-ion battery during rapid charge and discharge cycles," *J. Power Sources*, vol. 158, no. 1, pp. 535–542, Jul. 2006.

[17] M. Chen and G. A. Rincon-Mora, "Accurate electrical battery model capable of predicting runtime and IV performance," *IEEE Trans. Energy Convers.*, vol. 21, no. 2, pp. 504–511, Jun. 2006.

[18] A. Bocca, A. Sassone, D. Shin, A. Macii, E. Macii, and M. Poncino, "A temperature-aware battery cycle life model for different battery chemistries," in *Proc. IFIP/IEEE Int. Conf. Very Large Scale Integr. Syst. Chip*, 2015, pp. 109–130.

[19] S. Bashash, S. J. Moura, J. C. Forman, and H. K. Fathy, "Plug-in hybrid electric vehicle charge pattern optimization for energy cost and battery longevity," *J. Power Sources*, vol. 196, no. 1, pp. 541–549, Jan. 2011.

[20] C. Zhou, K. Qian, M. Allan, and W. Zhou, "Modeling of the cost of EV battery wear due to V2G application in power systems," *IEEE Trans. Energy Convers.*, vol. 26, no. 4, pp. 1041–1050, Dec. 2011.

[21] A. Ovalle, A. Hably, S. Bacha, G. Ramos, and J. Hossain, "Escort evolutionary game dynamics approach for integral load management of electric vehicle fleets," *IEEE Trans. Ind. Electron.*, vol. 64, no. 2, pp. 1358–1369, Feb. 2017.

[22] W. Tang and Y. J. A. Zhang, "A model predictive control approach for low-complexity electric vehicle charging scheduling: Optimality and scalability," *IEEE Trans. Power Syst.*, vol. 32, no. 2, pp. 1050–1063, Mar. 2017.

[23] F. Soares, P. R. Almeida, and J. P. Lopes, "Quasi-real-time management of electric vehicles charging," *Elect. Power Syst. Res.*, vol. 108, pp. 293–303, Mar. 2014.

[24] Z. Wei, Y. Li, Y. Zhang, and L. Cai, "Intelligent parking garage EV charging scheduling considering battery charging characteristic," *IEEE Trans. Ind. Electron.*, vol. 65, no. 3, pp. 2806–2816, Mar. 2018.
[25] T. Franke and J. F. Krems, "Understanding charging behaviour of electric vehicle users," *Transp. Res. Part F, Traffic Psychol. Behav.*, vol. 21, pp. 75–89, Nov. 2013.
[26] P. Palensky, E. Widl, M. Stifter, and A. Elsheikh, "Modeling intelligent energy systems: Co-simulation platform for validating flexible-demand EV charging management," *IEEE Trans. Smart Grid*, vol. 4, no. 4, pp. 1939–1947, Dec. 2013.
[27] D. Andersson and D. Carlsson, "Measurement of ABB's prototype fast charging station for electric vehicles," Master's thesis, Chalmers Univ. Technol., Gothenburg, Sweden, 2012.
[28] R. Spotnitz, "Simulation of capacity fade in lithium-ion batteries," *J. Power Sources*, vol. 113, no. 1, pp. 72–80, Jan. 2003.
[29] [Online]. Available: https://en.wikipedia.org/wiki/Arrhenius_equation. Accessed on: May 16, 2018.
[30] A. Hoke, A. Brissette, K. Smith, A. Pratt, and D. Maksimovic, "Accounting for lithium-ion battery degradation in electric vehicle charging optimization," *IEEE J. Emerg. Sel. Topics Power Electron.*, vol. 2, no. 3, pp. 691–700, Sep. 2014.
[31] O. Beaude, S. Lasaulce, M. Hennebel, and I. Mohand-Kaci, "Reducing the impact of EV charging operations on the distribution network," *IEEE Trans. Smart Grid*, vol. 7, no. 6, pp. 2666–2679, Nov. 2016.
[32] C.-Y. Chung, J. Chynoweth, C. Qiu, C.-C. Chu, and R. Gadh, "Design of fair charging algorithm for smart electrical vehicle charging infrastructure," in *Proc. IEEE Int. Conf. ICT Convergence*, 2013, pp. 527–532.
[33] L. Hua, J. Wang, and C. Zhou, "Adaptive electric vehicle charging coordination on distribution network," *IEEE Trans. Smart Grid*, vol. 5, no. 6, pp. 2666–2675, Nov. 2014.
[34] 2018. [Online]. Available: https://www.tesla.com/en_CA/models
[35] 2012. [Online]. Available: http://large.stanford.edu/courses/2012/ph240/landreman1/docs/2012-Nissan-LEAF.pdf
[36] R. Jain, *The Art of Computer Systems Performance Analysis: Techniques for Experimental Design, Measurement, Simulation, and Modeling*. Hoboken, NJ, USA: Wiley, 1990.
[37] B. Y. Liaw, E. P. Roth, R. G. Jungst, G. Nagasubramanian, H. L. Case, and D. H. Doughty, "Correlation of Arrhenius behaviors in power and capacity fades with cell impedance and heat generation in cylindrical lithium-ion cells," *J. Power Sources*, vol. 119, pp. 874–886, Jun. 2003.

Zhe Wei (S'15) received the B.Sc. and M.Sc. degrees in electrical engineering from Northwestern Polytechnical University, Xi'an, China, in 2009 and 2012, respectively, and the Ph.D. degree in electrical and computer engineering from the University of Victoria, Victoria, BC, Canada, in 2017. His research interests include electric vehicle charging scheduling, resource allocation, new energy vehicles, and intelligent transportation system.

Yue Li received the B.Sc. and M.Sc. degrees in electrical engineering from the Beijing Institute of Technology, Beijing, China, in 2006 and 2008, respectively. He is currently working toward the Ph.D. degree with the Department of Electrical and Computer Engineering, University of Victoria, Victoria, BC, Canada. From 2008 to 2013, he was with the Wireless Research Department, Huawei, as a standard Preresearch Engineer. He has been closely involved in 3GPP standards' evolvement and held numerous patents in WCMDA, LTE-A, and 5G systems. His research interests include next-generation cellular system, wireless network design and optimization, wireless system modeling, and performance analysis.

Lin Cai (S'00–M'06–SM'10) received the M.A.Sc. and Ph.D. degrees in electrical and computer engineering from the University of Waterloo, Waterloo, ON, Canada, in 2002 and 2005, respectively. Since 2005, she has been with the Department of Electrical and Computer Engineering, University of Victoria, Victoria, BC, Canada, where she is currently a Professor. Her research interests span several areas in communications and networking, with a focus on network protocol and architecture design supporting emerging multimedia traffic over wireless, mobile, *ad hoc*, and sensor networks.

She was a TPC Symposium Co-Chair for IEEE Globecom'10 and Globecom'13. She was an Associate Editor for the IEEE TRANSACTIONS ON WIRELESS COMMUNICATIONS, the IEEE TRANSACTIONS ON VEHICULAR TECHNOLOGY, *EURASIP Journal on Wireless Communications and Networking*, *International Journal of Sensor Networks*, and *Journal of Communications and Networks*, and was the Distinguished Lecturer of the IEEE VTS Society. She was the recipient of the NSERC Discovery Accelerator Supplement Grants in 2010 and 2015, respectively, and the Best Paper Awards of IEEE ICC 2008 and IEEE WCNC 2011. She has founded and chaired the IEEE Victoria Section Vehicular Technology and Communications Joint Societies Chapter.